Self-Organized Nanotemplating on Misfit Dislocation Networks Investigated by Scanning Tunneling Microscopy

BOGDAN DIACONESCU,* GEORGI NENCHEV, JOSHUA JONES, AND KARSTEN POHL
Department of Physics and Materials Science Program, University of New Hampshire, Durham, New Hampshire 03824

KEY WORDS self-assembly; STM; strained metallic interfaces; ultrathin films; misfit dislocation network

ABSTRACT Self-ordering growth of nanoarrays on strained metallic interfaces is an attractive option for preparing highly ordered nanotemplates. The great potential of this natural templating approach is that symmetry, feature sizes, and density are predicted to depend on the interfacial stress in these strained layers, which can be adjusted by changing the substrate-thin film composition, temperature, and adlayer coverage. This bottom-up approach of growing nanostructured two-dimensional ordered arrays of clusters on the misfit dislocation networks of strained metallic thin films and surfaces requires a detailed understanding of the nucleation and film–adsorbate interaction processes. Here we show how high resolution, large scale, variable temperature scanning tunneling microscopy imaging can improve our understanding of these self-assembly processes. *Microsc. Res. Tech. 70:547–553, 2007.*

INTRODUCTION

Ultrathin metal films have been observed to form ordered arrays of dislocation structures to relieve the strain caused by the different lattice spacing between the adsorbate film and substrate (Barth et al., 1990; Günther et al., 1995; Hwang et al., 1995). Such ordered misfit dislocation networks are particularly interesting as templates for self-assembly of arrays of nanoclusters (Brune et al., 1998; Chambliss et al., 1991a; Helveg et al., 2000) with novel properties. It is expected that these structures find application in higher density magnetic storage, more selective catalysis, and higher sensitivity biochemical sensors, and, perhaps, quantum computing and photonics. However, the controlled fabrication of such nanoarrays with reproducible properties is a serious challenge, and surface science has to play a key role in the understanding of their formation and their characterization. The complexity of the problem resides in the large number of atoms involved in such reconstructions, because unit cell sizes of the strained two-dimensional networks often contain few hundreds to thousands of atoms. To understand these self-assembly processes, very large scale, atomically resolved, and variable temperature scanning tunneling microscopy (VT-STM) data need be linked via atomistic models with first-principles information about the system. We have therefore designed and home-built a VT-STM instrument capable of large scale, high speed, variable temperature atomically resolved STM imaging of compact metal surfaces (Diaconescu et al., submitted). The great potential of this template approach in strained thin films is that the feature sizes and symmetry are believed to be tunable by controlling the misfit (Alerhand et al., 1988; Marchenko, 1981). This can be achieved, e.g., by adjusting the misfit between the ultrathin film and substrate, or by controlling the coverage or temperature. Also, the chemistry of the adsorbates on these strained metallic interfaces can strongly affect the final equilibrium state of the multicomponent systems.

2D MISFIT DISLOCATION NETWORKS

In general, growth of a thin film on a dissimilar substrate results in a strained interface due to the lattice mismatch between the two materials. Strain is often partially relieved through the formation of well-ordered networks of misfit dislocations (Günther et al., 1995).

Au(111) Misfit Dislocation Network; Basic Elements

The herringbone reconstruction of Au(111) is an example how an ordered misfit dislocation network can also form on a clean surface. Cleaving a Au crystal along the (111) crystallographic plane should leave a FCC terminated surface. Experimental observations (Barth et al., 1990) have shown that, however, terminating a Au crystal in a (111) surface leaves the top layer in compression by 4% with respect to the layers below due to the accommodation of additional Au atoms, resulting in three possible 120° rotated domains of a zig-zag like reconstruction pattern shown in Figure 1a (Narasimhan and Vanderbilt, 1992; Takeuchi et al., 1991). The basic elements of such a system are: (i) Shockley partial dislocations consisting of Au atoms sitting on bridge sites along one of the threefold symmetric $\sqrt{3}$, or $[11\bar{2}]$, directions, at the boundary of consecutive FCC and HCP stacking of the top layer Au atoms (Fig. 1b), and (ii) threading dislocations (TDs) normal to the surface plane formed at the meeting

*Correspondence to: Bogdan Diaconescu, Department of Physics, University of New Hampshire, Durham, New Hampshire 03824.
E-mail: bogdan@einstein.unh.edu

Present address of Joshua Jones: Andover Corporation, Salem, New Hampshire 03079.

Received 5 February 2007; accepted in revised form 15 February 2007

Contract grant sponsor: National Science Foundation and Center for High-Rate Nanomanufacturing; Contract grant numbers: DMR-0134933 and NSF-0425826.

DOI 10.1002/jemt.20479

Published online 4 May 2007 in Wiley InterScience (www.interscience.wiley.com).

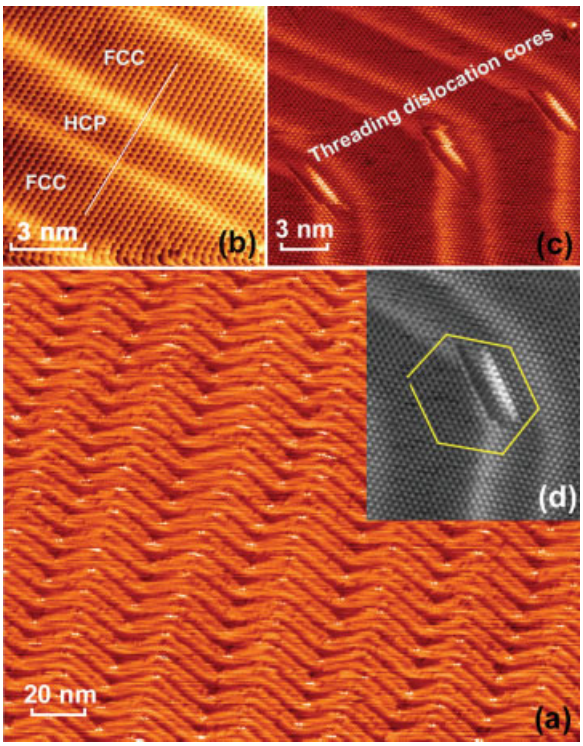

Fig. 1. Constant current image of Au(111): (**a**) large scale misfit dislocation network; (**b**) inset showing atomically resolved Shockley partial dislocations as bright stripes with alternating FCC-HCP-FCC areas bounded by atoms sitting on the bridge sites along $[11\bar{2}]$ directions; the white straight line shows how the stacking of the Au atoms changes as it passes across the Shockley partials; (**c**) treading dislocation cores formed where two Shockley partial dislocations meet; (**d**) Burger circuit around a threading dislocation core showing one extra row of atoms.

point of two Shockley partial dislocations shown in Figure 1c. The top Au atomic layer is in registry with the substrate in the $\sqrt{3}$ direction while it is compressed along the close-packed directions where 23 Au atoms sit on top of 22 Au atoms of the substrate. The hexagonal symmetry of the nearest neighbors is maintained everywhere with the exception of the treading dislocation core sites, seen in Figure 1d as the bright rows of atoms at the elbow sites, where a Burger vector circuit shows the existence of an extra row of atoms. The rectangular unit cell size of the reconstruction is about 8.5 nm × 35 nm.

The only other known clean metal surface to reconstruct in a misfit dislocation network is the (111) surface of platinum, which exhibits a similar reconstruction (Bott et al., 1993). Both surfaces exhibit the reconstruction due to the misfit of the lattice spacing in the thin film and bulk substrate. Many semiconductor surfaces also reconstruct at room temperature, however, the presence of dangling bonds at the surface makes these systems chemically and structurally less stable.

Misfit Dislocation Networks of 1 ML Ag/Ru(0001)

The size and symmetry of the dislocation networks on single crystal metal surfaces cannot be altered. For viable template solutions we have to focus on systems where we can engineer unique dislocation networks,

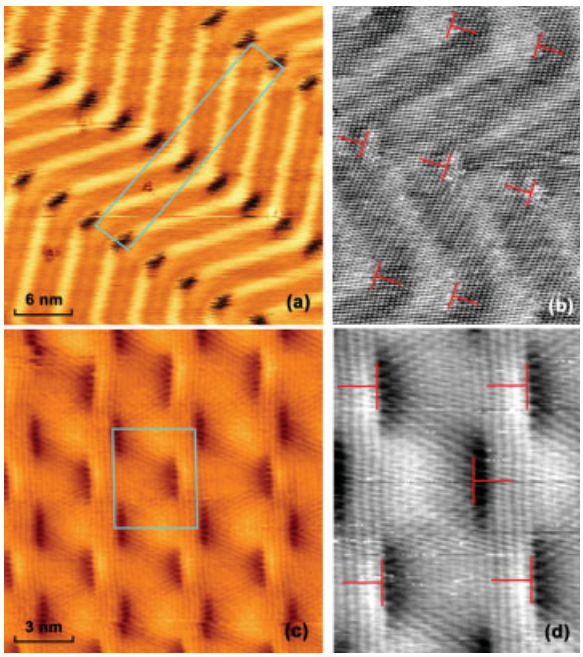

Fig. 2. Constant current STM images of the reconstructions of 1 atomic layer Ag film on Ru(0001): (**a**) large Herring Bone (LHB) network at 295 K and overall Ag coverage larger than 1 ML normalized to Ru(0001) substrate; (**b**) inset showing atomically resolved LHB-Shockley partial dislocations are running between consecutive, alternate orientations of the treading dislocation cores, which are marked by red "T"s; (**c**) Short Herring Bone (SHB) network at 110 K and overall Ag coverage less than 1 ML; (**d**) atomically resolved inset of the unit cell of the SHB network from (c).

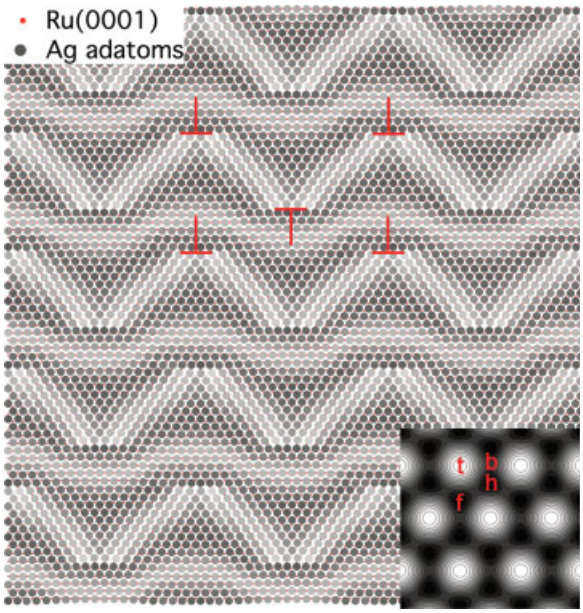

Fig. 3. 2D Frenkel–Kontorova model of the misfit dislocation network of 0.x ML Ag/Ru(0001), the short herringbone (SHB) structure; the inset shows the surface potential obtained from the first principles results of the binding energies of Ag on Ru(0001) at the high symmetry points: $E_t = 282$ meV (top), $E_b = 55$ meV (bridge), and $E_h = E_f = 0$ (HCP and FCC sites). Ag-Ag interaction parameters are the elastic constant of the Ag film, $k = 2000$ meV/Å^2 and the lattice mismatch $b = a_{Ag}/a_{Ru} = 1.14$. The gray level is proportional to the surface potential at the location of each Ag atom, and thus indicates its relative height.

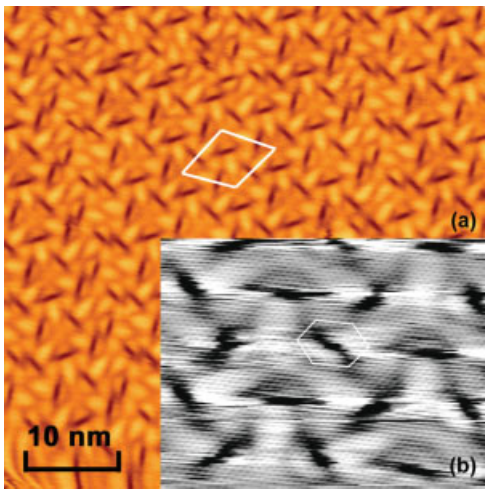

Fig. 4. Constant current STM images of the trigon reconstruction of 2 atomic layer Ag/Ru(0001): (**a**) large scale image with the primitive unit cell of the superstructure marked with white lines; (**b**) atomically resolved image showing that the symmetry of the top layer is hexagonal everywhere. The closed burger vector circuit shows no threading dislocation is present at the darker regions. [Color figure can be viewed in the online issue, which is available at www.interscience.wiley.com.]

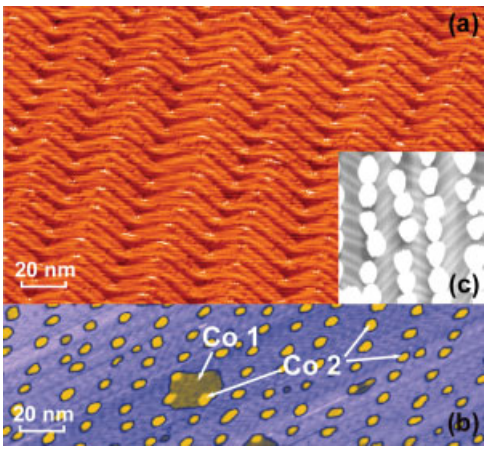

Fig. 5. Selective adsorbtion of Co on Au(111): (**a**) misfit dislocation network of Au(111); (**b**) Co clusters grown on Au(111); Co nucleates mostly in 2 atomic layer thick clusters of few tens of atoms at the threading dislocation sites of Au(111), Co 2, with some clusters being only one atomic layer high, Co 1; (**c**) enhanced contrast showing the location of the nucleation of Co clusters at the threading dislocation cores; Au(111) is unaffected by Co seen by the existence of the Shockley partial dislocations. All STM data at 295 K. [Color figure can be viewed in the online issue, which is available at www.interscience.wiley.com.]

i.e., thin film interfaces of dissimilar materials with adjustable strain caused by lattice mismatch, coverage, and temperature.

An excellent model system to test the effect of coverage and temperature on the misfit dislocation network is monolayer thick Ag film on Ru(0001) (Hwang et al., 1995; Ling et al., 2006). By contrast to the Au(111) misfit dislocation network, for a 1 atomic layer thick Ag film on Ru(0001) the Ag adlayer is expanded relative to the surface layer of Ru(0001) due to a lower atom density in the Ag layer than in the Ru(0001) plane. The lattice spacing of bulk Ag is about 7% larger than that of bulk Ru. For a coverage slightly larger than 1 ML, the misfit dislocation of 1 atomic layer thick Ag film on Ru(0001) has a unit cell size of $a \times c = 68(70) \times 16(17)$ Ag atoms called Long Herring Bone (LHB), shown in Figure 2a and 2b, where the Shockley partial dislocations are running along $\sqrt{3}$ directions like in the case of Au(111). At a coverage less than one monolayer, Ag film on Ru(0001) reconstruction changes into a misfit dislocation network with a unit cell size of $18(19) \times 15(16)$ Ag atoms called Short Herring Bone (SHB), as shown in STM data in Figures 2c and 2d. The dislocation structure of SHB and LHB reconstructions is similar, with a rectangular unit cell, but different lengths and orientations of Shockley partial dislocations running between TD cores. The LHB structure formed for 1.x ML Ag coverage is not stable at high temperatures. As the temperature is increased above 480 K, LHB transforms into SHB reconstruction (Ling et al., 2006). The transition is reversible.

Misfit dislocation networks can be understood in the framework of a 2D Frenkel–Kontorova model (Hamilton, 1997; Hamilton et al., 1999; Hamilton and Foiles, 1995; Thürmer et al., 2004, 2006) where one has to consider the potential landscape of the surface seen by an adatom and the interadatom potential. The interactions within the adsorbate film and with the surface is described by the Hamiltonian

$$H = U_{\text{sub}} + U_{\text{Ag-Ag}} + \text{KE}.$$

If we neglect the kinetic energy term KE we have

$$H = \sum_{\vec{r}_i} \sum_{\vec{g}} V_{\vec{g}}\, e^{i\vec{g}\,\vec{r}_i} + \frac{k}{2} \sum_{\vec{r}_i} \sum_{\vec{r}_i \neq \vec{r}_j} \left(\left| \vec{r}_i - \vec{r}_j \right| - b a_{\text{Ru}} \right)^2$$

where k is the elastic constant of the Ag film and b is the lattice mismatch. This Hamiltonian can be solved for appropriate boundary conditions and density of the adsorbate layer to obtain the ground state solution. The result of such a simulation is shown in Figure 3, which closely describes the low temperature STM measurement in Figure 2c. The substrate potential landscape shown in the inset of Figure 3 is obtained by symmetry arguments from the binding energies of a Ag atom on high symmetry sites of Ru(0001), from first-principle calculations (Thayer et al., 2002).

Misfit Dislocation Networks of 2 ML Ag/Ru(0001)

We have seen how coverage and temperature can change the size of the unit cell of the misfit dislocation network for the case of 1 atomic layer thick Ag films on Ru(0001), while the rectangular symmetry of the unit cell of the reconstruction was maintained. In the case of 2 atomic layer thick Ag films on Ru(0001) the reconstruction has a trigonal symmetry, as shown by the STM image in Figure 4. The unit cell of the reconstruction runs between the centers of neighboring trigons in the $\sqrt{3}$ directions. The unit cell size is about $13\sqrt{3}$ nearest neighbor distances of the Ag layer. A key feature is the absence of TDs on the top layer, the darker, linear regions in the STM images corresponding to vertical displacements at the TDs in the first Ag layer,

thus the strain being accommodated in the first Ag layer (Ling et al., 2004).

GROWTH MECHANISMS OF 2D NANOCLUSTER ARRAYS ON MISFIT DISLOCATION NETWORKS

The availability of three parameters—lattice misfit, coverage, and temperature—in controlling the misfit dislocation network symmetry and characteristic size creates opportunities for the growth of two-dimensional arrays of clusters with various specific sizes onto such strained surfaces. The misfit dislocation network can play a passive role as in the case of adsorbates nucleating at specific sites or regions without changing its structure, or they can actively interact with the adsorbates, thus generating a completely new symmetry and periodicity of the multiphase system. In the following, we will show how different growth processes can lead to diverse 2D cluster-array sizes and symmetries.

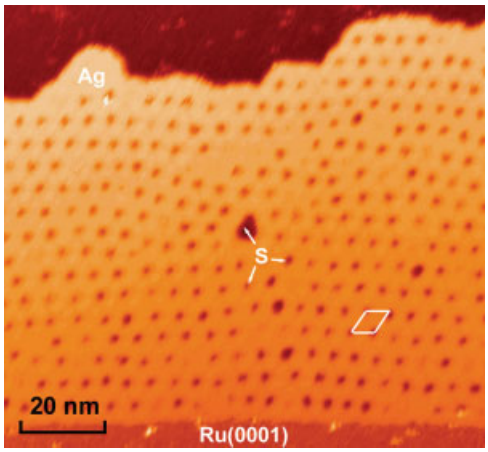

Fig. 6. S etching induced restructuring of the 1 atomic layer of Ag/Ru(0001). A new triangular symmetry of the superstructure is formed with S-filled vacancy islands 50 Å apart. [Color figure can be viewed in the online issue, which is available at www.interscience.wiley.com.]

Nucleation of Ad-Clusters at the TD Cores

An example for the passive role of the misfit dislocation network in the growth process of the adsorbates is Co cluster growth on Au(111) (Fruchart et al., 1999; Voigtländer et al., 1991). In this case, Au(111) serves as a template on which Co atoms nucleate at the TD sites leaving the reconstructed surface of Au(111) relatively undistorted, as seen by the existence of Shockley partial dislocations in Figure 5c. The symmetry and Co cluster spacing is thus following the symmetry and characteristic length scale of the substrate, as seen in Figures 5a and 5b. Most Co clusters have been observed to grow two atomic layers high and are seen as bright clusters in Figure 5b. One atomic layer height clusters are growing between them if Co coverage becomes higher than about 0.2 ML. Similar growth modes have also been observed for Fe (Stroscio et al., 1992) and Ni (Chambliss et al., 1991a,b), Mo and Ru adsorbed on Au(111).

Adsorbate-Induced Strain Relaxation of Misfit Dislocation Networks

Deposition of molecular sulfur from an electrochemical cell (Xu and Hrbeck, 1989) onto LHB and SHB reconstructed surfaces of Ag/Ru(0001) at room temperature generates a well-ordered array of sulfur-filled Ag vacancies islands (Pohl et al., 1999; Thürmer et al., 2004, 2006). The three-phase system composed of S, 1 atomic layer Ag and Ru(0001) forms a well-ordered two-dimensional array of uniformly spaced S clusters embedded into the Ag film, as shown in Figure 6. The cluster array shows a triangular lattice with an average distance between clusters of about 4.5 nm.

We performed detailed STM studies of the growth process as a function of S coverage for SHB of Ag/Ru(0001) and found a two-stage process. At low S coverage, individual vacancies with a fixed size are formed, their density increases proportionally with the sulfur coverage until an almost complete array of vacancies is formed. After S coverage exceeds the threshold values of <18 mML the S-filled vacancy

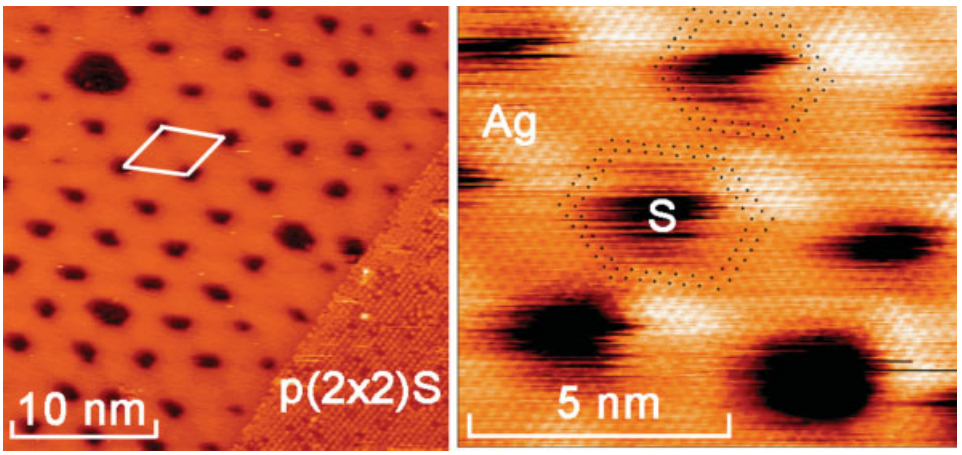

Fig. 7. S etching induced restructuring of the SHB of Ag/Ru(0001) ($T = 295$ K): (right) no threading dislocations are left in the Ag film after S etching; (left) new triangular symmetry of the superstructure with S-filled vacancy islands 50 Å apart. [Color figure can be viewed in the online issue, which is available at www.interscience.wiley.com.]

islands start growing in size. An intriguing aspect is that the Ag vacancy islands saturation density is exactly half of the surface density of the TD of SHB of Ag/Ru(0001). Another key finding is the restructuring of the Ag film occurring after the S etching process: (i) a change of the symmetry of the unit cell size and (ii) the absence of TDs in the Ag film shown by the absence of a nonzero Burger vector (Fig. 7). Inside a unit cell there are two equivalent positions that can be occupied by the Ag vacancy island, the black and white dots marked in Figure 8, thus two hexagonal equivalent lattices can be formed following the S etching restructuring process. Such a mechanism naturally generates the new symmetry and also explains the other experimental observations: (i) the conservation of the unit cell area of 21.4 nm^2 for Ag/Ru(0001) versus 21.6 nm^2 for S/Ag/Ru(0001), and (ii) the 2:1 ratio of TDs and Ag vacancies (Diaconescu and Pohl, to be published).

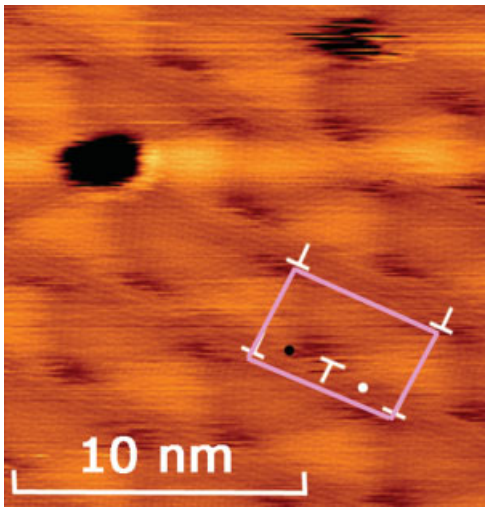

Fig. 8. STM image at 150 K of the initial S etching of SHB of Ag/Ru(0001) process showing two S-filled Ag vacancy islands. There are two equivalent etching sites per primitive unit cell, which are marked with black and white dots, each of the S-filled vacancies in the image residing on one of them. [Color figure can be viewed in the online issue, which is available at www.interscience.wiley.com.]

The striking transformation of both misfit dislocation networks of Ag into a similar final structure requires the rearrangement of large numbers of atoms and also a different mechanism through which the strain is relieved. In the case of S adsorbed on LHB misfit dislocation network, Thürmer et al. (2004) have shown how the strain relaxation mechanism involved in the formation of S-filled Ag vacancies array can be explained in two steps. The first step involves the formation of S-filled Ag vacancy islands at the TD core, followed by the creation of adjacent triangular patches of Ag film with alternating FCC and HCP stacking. The second step involves creation of S-filled Ag vacancies at their corners and followed by climb and annihilation of dislocations. In the case of S etching SHB, the mechanism involves a TD pair annihilation process, followed by a glide of Shockley partial dislocations. While S etching of LHB networks involves a reshuffling of a large number of atoms, in the case of S self-assembly on SHB networks, the self-assembly process is a local one involving mainly atoms in a SHB primitive unit cell.

Another example of chemical induced restructuring of a misfit dislocation network is S adsorbed on 2 atomic height Cu films on Ru(0001) (de la Figuera et al., 2003; Hrbek et al., 1999). While nucleation of metallic adatoms on misfit dislocation networks usually generates circular shaped clusters, S adsorbed on the stripe misfit dislocation of 2 ML Cu/Ru(0001) generates linear shaped S clusters of seven S atoms. They are forming the sides of equilateral triangles sitting at the TD sites of Cu, with a trigon like symmetry, shown in Figure 9.

Limited Diffusion Nucleation

These strained metallic interfaces can also be used to selectively adsorb and nucleate organic molecules such

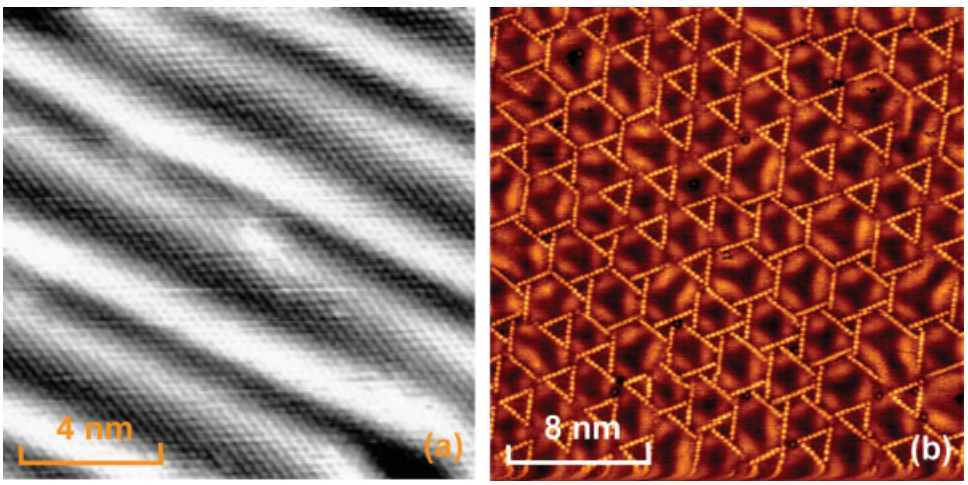

Fig. 9. Sulfur-induced reconstruction (**b**) of the stripe misfit dislocation network of 2 ML Cu/Ru(0001) (**a**). S atoms are seen as linear bright arrays with an overall threefold symmetry (b). STM data taken at 295 K. [Color figure can be viewed in the online issue, which is available at www.interscience.wiley.com.]

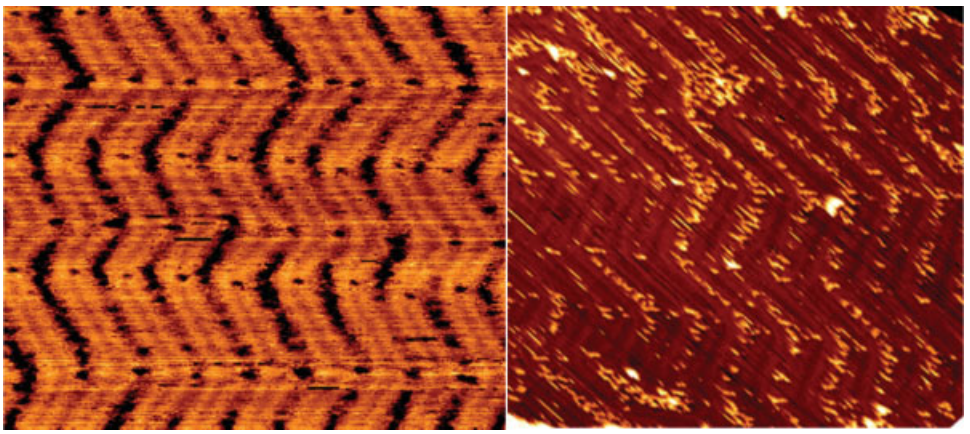

Fig. 10. Selective nucleation of CH_3SH molecules on the FCC sites of the misfit dislocation network of Au(111) at 150 K. Left STM image is taken in negative contrast mode with the nucleated islands of CH_3SH showing darker than Au(111); the right hand side STM image is in positive contrast mode showing CH_3SH clusters brighter than Au(111). [Color figure can be viewed in the online issue, which is available at www.interscience.wiley.com.]

as methanethiol on the FCC sites between the Shockley partial dislocations (Fig. 10) (Nenchev et al., to be published). Pattern in methanethiol self-assembled monolayers (SAMs) (Fitts et al., 2002; Maksymovych et al., 2006; Poirier and Pylant, 1996) forms as a 2D imprint of ordered Co cluster-array grown on the herringbone pattern of Au(111). This cluster-array and dislocation pattern imprinting process can be applied to a wide variety of sulfur-containing molecular films. This method enables the patterning of SAMs and ultimately the ordering of desired nanoelements such as carbon nanotubes and proteins.

CONCLUSION

Well-ordered misfit dislocation networks of thin metal films are a viable candidate for growth of two-dimensional ordered nanocluster arrays with specific symmetries, feature size, and lattice spacing. Such bottom-up processes can be very complex involving collective effects from large numbers of atoms. Understanding of these self-assembly processes requires detailed experimental information at the atomic level of large ensembles of hundreds to thousands of atoms, and thus large-scale VT-STM imaging is an essential tool for such studies.

REFERENCES

Alerhand OL, Vanderbilt D, Meade RD, Joannopoulos JD. 1988. Spontaneous formation of stress domains on crystal surfaces. Phys Rev Lett 61:1973–1976.

Barth JV, Brune H, Ertl G, Behm RJ. 1990. Scanning tunneling microscopy observations on the reconstructed Au(111) surface: Atomic structure, long-range superstructure, rotational domains, and surface defects. Phys Rev B 42:9307–9318.

Bott M, Hohage M, Michely T, Comsa G. 1993. Pt(111) reconstruction induced by enhanced Pt gas-phase chemical potential. Phys Rev Lett 70:1489–1492.

Brune H, Giovannini M, Bromann K, Kern K. 1998. Self-organized growth of nanostructure arrays on strain-relief patterns. Nature 394:451–453.

Chambliss DD, Wilson RJ, Chiang S. 1991a. Nucleation of ordered Ni island array on Au(111) by the surface-lattice dislocations. Phys Rev Lett 66:1721–1724.

Chambliss DD, Wilson RJ, Chiang S. 1991b. Ordered nucleation of Ni and Au islands on Au(111) studied by scanning tunneling microscopy. J Vac Sci Technol B 9:933–937.

de la Figuera J, Carter CB, Bartelt NC, Hwang QR. 2003. Interplay between gas adsorption and dislocation structure on a metal surface. Surf Sci 531:29–38.

Diaconescu B, Pohl K. (to be published).

Diaconescu B, Nenchev G, de la Figuera J. An ultra high vacuum fast scanning and variable temperature scanning tunneling microscope for large scale imaging (submitted).

Fitts WP, White JM, Poirier EG. 2002. Low-coverage decanethiolate structure on Au(111): Substrate effects. Langmuir 18:1561–1566.

Fruchart O, Klaua M, Barthel J, Kirschner J. 1999. Self-organized growth of nanosized vertical magnetic Co pillars on Au(111). Phys Rev Lett 83:2769–2772.

Günther C, Vrijmoeth J, Hwang RQ, Behm JR. 1995. Strain relaxation in hexagonally close-packed metal-metal interfaces. Phys Rev Lett 74:754–757.

Hamilton CJ. 1997. Dislocation nucleation rates during submonolayer growth of heteroepitaxial thin films. Phys Rev B 55:R7402–R7405.

Hamilton JC, Foiles MS. 1995. Misfit dislocation structure for close-packed metal–metal interfaces. Phys Rev Lett 75:882–885.

Hamilton JC, Stumpf R, Bromann K, Giovannini M, Kern K, Brune H. 1999. Dislocation structures of submonolayer films near the commensurate–incommensurate phase transition: Ag on Pt(111). Phys Rev Lett 82:4488–4491.

Helveg SS, Lauritsen JV, LÌgsgaard E, Stensgaard I, Nørskov JK, Clausen BS, Topsøe H, Besenbacher F. 2000. Atomic-scale structure of single-layer MoS_2 nanoclusters. Phys Rev Lett 84:951–954.

Hrbek J, de la Figuera J, Pohl K, Jirsak T, Rodriguez JA, Schmid AK, Bartelt NC, Hwang QR. 1999. A prelude to surface chemical reaction: Imaging the induction period of sulfur interaction with a strained Cu layer. J Phys Chem B 103:10557–10561.

Hwang RQ, Hamilton JC, Stevens JL, Foiles MS. 1995. Near-surface buckling in strained metal overlayer systems. Phys Rev Lett 75:4242–4245.

Ling WL, de la Figuera J, Bartelt NC, Hwang RQ, Schmid AK, Thayer GE, Hamilton CJ. 2004. Strain relief through heterophase interface reconstruction: Ag(111)/Ru(0001). Phys Rev Lett 92:116102-1–116102-4.

Ling WL, Hamilton JC, Thürmer K, Thayer G, de la Figuera J, Hwang R, Carter C, Bartelt N, McCarty K. 2006. Herringbone and triangular patterns of dislocations in Ag, Au, and AgAu alloy films on Ru(0001). Surf Sci 600:1735–1757.

Maksymovych P, Sorescu DC, John J, Yates T. 2006. Gold-adatom-mediated bonding in self-assembly short-chain alkanethiolate species on the Au(111) surface. Phys Rev Lett 97:146103-1–146103-4.

Marchenko IV. 1981. Possible structures and phase transitions on the surface of crystals. Sov Phys JETP Lett 33:381–383.

Narasimhan S, Vanderbilt D. 1992. Elastic stress domains and the herringbone reconstruction on Au(111). Phys Rev Lett 69:1564–1567.

Pohl K, Bartelt MC, de la Figuera J, Bartelt NC, Hrbek J, Hwang R. 1999. Identifying the forces responsible for self-organization of nanostructures at crystal surfaces. Nature 397:238–241.

Poirier GE, Pylant DE. 1996. The self-assembly mechanism of alkenethiols on Au(111). Science 272:1145–1148.

Stroscio JA, Pierce DT, Dragoset AR, First NP. 1992. Microscopic aspects of the initial growth of metastable fcc iron on Au(111). J Vac Sci Technol A 10:1981–1985.

Takeuchi N, Chan CT, Ho MK. 1991. Au(111): A theoretical study of the surface reconstruction and the surface electronic structure. Phys Rev B 43:13899–13906.

Thayer GE, Bartelt NC, Ozolins V, Schmid AK, Chiang S, Hwang QR. 2002. Linking surface stress to surface structure: Measurement of atomic strain in a surface alloy using scanning tunneling microscopy. Phys Rev Lett 89:036101–036105.

Thürmer K, Carter CB, Bartelt NC, Hwang QR. 2004. Self-assembly via adsorbate-driven dislocation reactions. Phys Rev Lett 92: 106101–106104.

Thürmer K, Carter CB, Bartelt NC, Hwang QR. 2006. Surface self-organization caused by dislocation networks. Science 311:1272–1274.

Voigtländer B, Meyer G, Amer NM. 1991. Epitaxial growth of thin magnetic cobalt films on Au(111) studied by scanning tunneling microscopy. Phys Rev B 44:10354–10357.

Xu GQ, Hrbeck J. 1989. New adsorption states of hydrogen on sulfur modified Ru(001). Catal Lett 2:35–41.